Coating microchannels to improve Field-Flow Fractionation

Tyler Shendruk
Gary Slater

September 12, 2011

Normal-mode Field Flow Fractionation

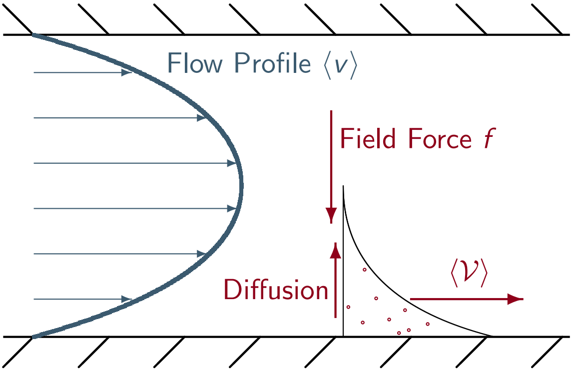

Figure: Schematic of normal-mode FFF.

Normal-mode Field Flow Fractionation

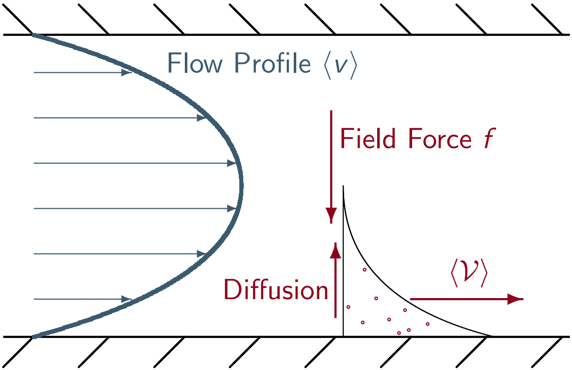

Figure: Schematic of normal-mode FFF.

Fractionation

$$\lambda \equiv \frac{k_B T}{f w}$$

Normal-mode Field Flow Fractionation

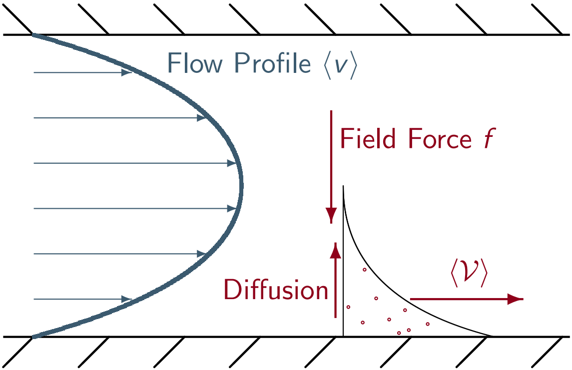

Figure: Schematic of normal-mode FFF.

Fractionation

$$\lambda \equiv \frac{k_B T}{f w}$$

$$c(\tilde{y}) = c_0 e^{-\tilde{y}/\lambda}$$

Normal-mode Field Flow Fractionation

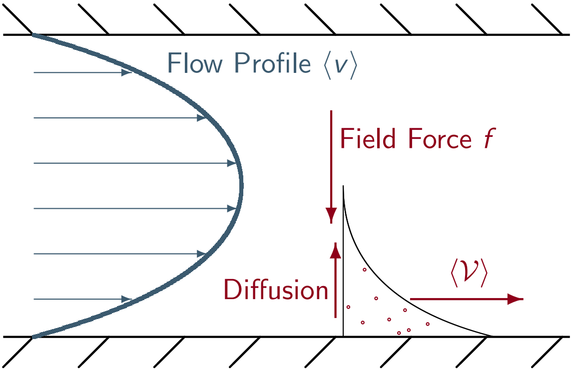

Figure: Schematic of normal-mode FFF.

Fractionation

$$\lambda \equiv \frac{k_B T}{f w}$$

$$c(\tilde{y}) = c_0 e^{-\tilde{y}/\lambda}$$

$$\langle \mathcal{V} \rangle = \frac{\langle c v \rangle}{\langle c \rangle}$$

Normal-mode Field Flow Fractionation

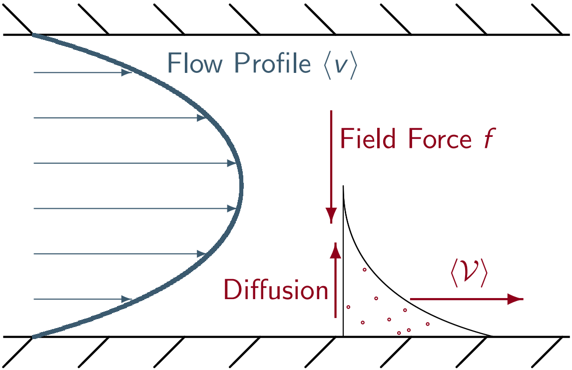

Figure: Schematic of normal-mode FFF.

Fractionation

$$\lambda \equiv \frac{k_B T}{fw}$$

$$c(\tilde{y}) = c_0 e^{-\tilde{y}/\lambda}$$

$$\langle\mathcal{V}\rangle = \frac{\langle cv\rangle}{\langle c\rangle}$$

$$R \equiv \frac{\langle\mathcal{V}\rangle}{\langle v\rangle}$$

Steric-mode Field Flow Fractionation

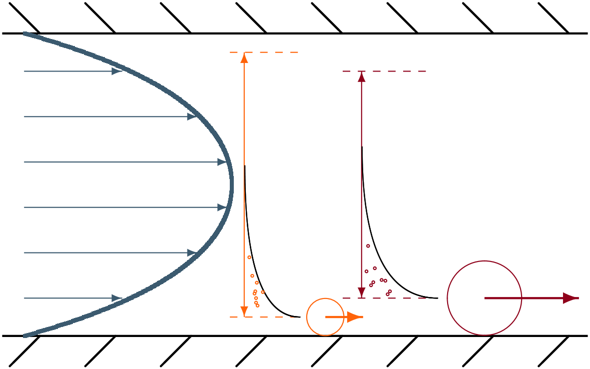

Figure: Schematic of steric-mode FFF.

Steric-mode Field Flow Fractionation

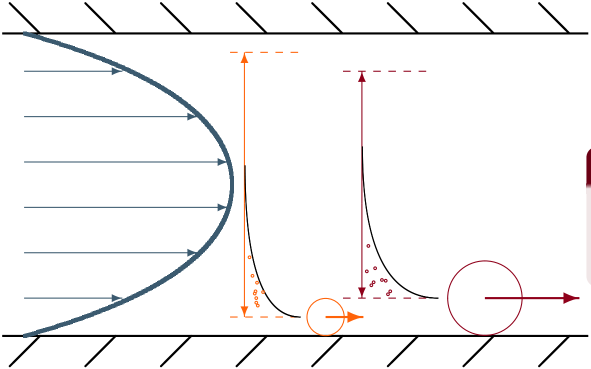

Figure: Schematic of steric-mode FFF.

Excluded Region

$$c(\tilde{y}) = \begin{cases} c_0 e^{-(\tilde{y}-\tilde{r})/\lambda} & \text{for } \tilde{r} < \tilde{y} < 1-\tilde{r} \\ 0 & \text{otherwise.} \end{cases}$$

Selective-mode Field Flow Fractionation

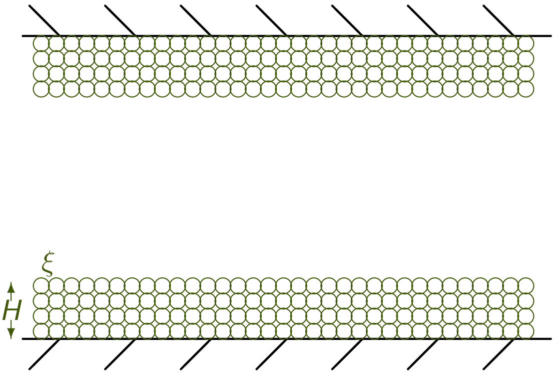

Figure: Schematic of selective-mode FFF.

Polymer Brush

Selective-mode Field Flow Fractionation

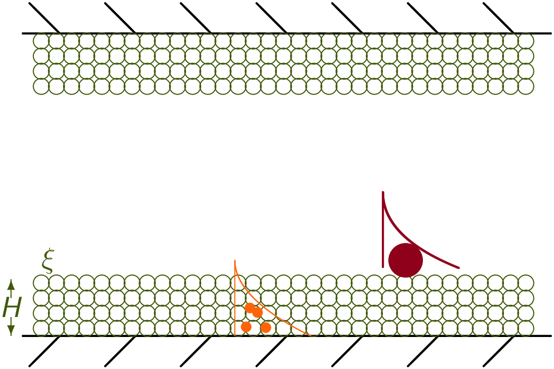

Figure: Schematic of selective-mode FFF.

Polymer Brush

- Free energy cost

Selective-mode Field Flow Fractionation

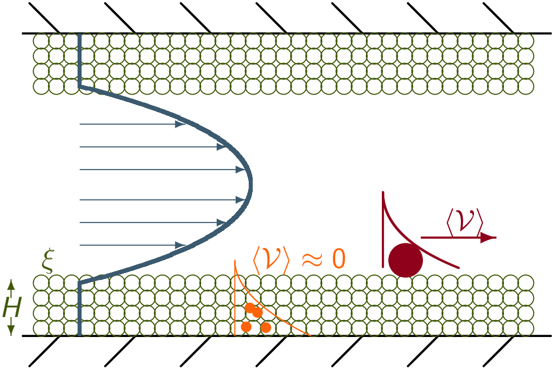

Figure: Schematic of selective-mode FFF.

Polymer Brush

- Free energy cost
- Hydrodynamic thickness

Selective-mode Field Flow Fractionation

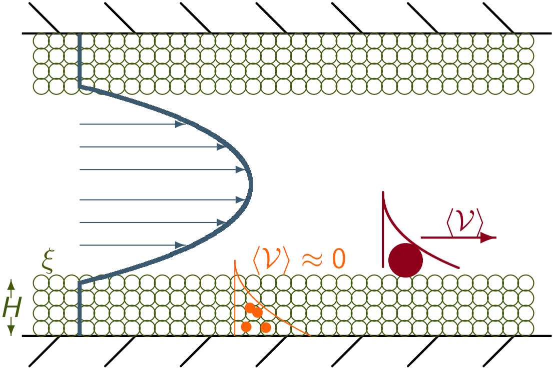

Figure: Schematic of selective-mode FFF.

Polymer Brush

- Free energy cost
- Hydrodynamic thickness

Brush Model

- Alexander Brush
  - step-function model

Flow Profile

Brush Model

- Alexander Brush
  - porous: blob size sets permeability
- Brinkman Equation

$$\eta \nabla^2 v + \frac{\eta}{\xi^2} v = \nabla p$$

Flow Profile

Brush Model

- Alexander Brush
  - porous: blob size sets permeability
- Brinkman Equation

$$\eta\nabla^2 v + \frac{\eta}{\xi^2} v = \nabla p$$

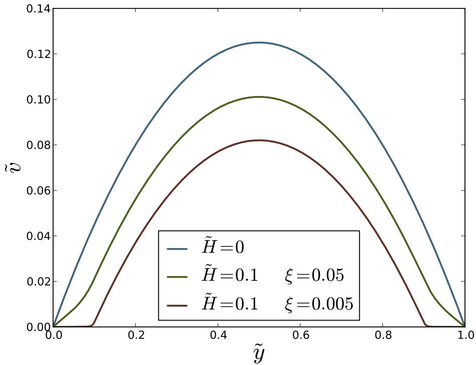

Modes of Approach

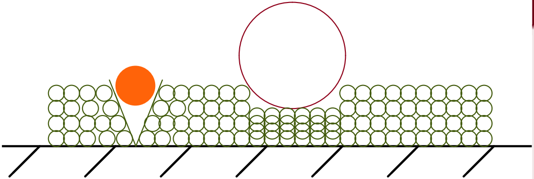

Figure: Two modes of approach.

Compression Mode

$$F_{\text{cmp}} = F_{\text{int}} + F_{\text{el}}$$
$$\approx F_0 \left[\left(\frac{H}{h} \right)^{\frac{1}{3\nu - 1}} + \left(\frac{h}{H} \right)^{\frac{4\nu - 1}{3\nu - 1}} \right]$$

where $F_0 = H/\xi$.

Modes of Approach

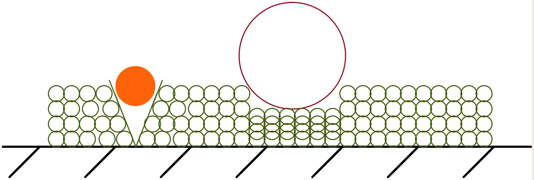

Figure: Two modes of approach.

Insertion Mode

Generally,

$$F_{\text{ins}} = \Pi(\phi)V + \gamma(\phi)A$$

Modes of Approach

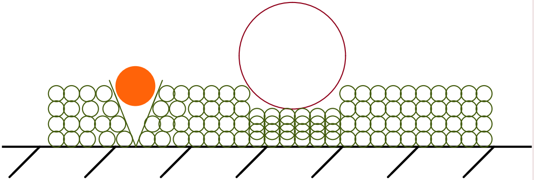

Figure: Two modes of approach.

Insertion Mode

Generally,

$$F_{\text{ins}} = \Pi(\phi)V + \gamma(\phi)A$$

When $r > \xi$

$$\frac{F_{\text{ins}}}{k_B T} \sim \left(\frac{r}{\xi}\right)^3 \left[1 + \frac{\xi}{r}\right]$$

Modes of Approach

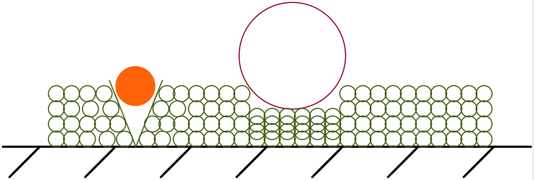

Figure: Two modes of approach.

Insertion Mode

Generally,

$$F_{\text{ins}} = \Pi(\phi)V + \gamma(\phi)A$$

When $r > \xi$

$$\frac{F_{\text{ins}}}{k_B T} \sim \left(\frac{r}{\xi}\right)^3 \left[1 + \frac{\xi}{r}\right]$$

When $r < \xi$

$$\frac{F_{\text{ins}}}{k_B T} \sim \left(\frac{r}{\xi}\right)^{3-1/\nu}$$

Modes of Approach

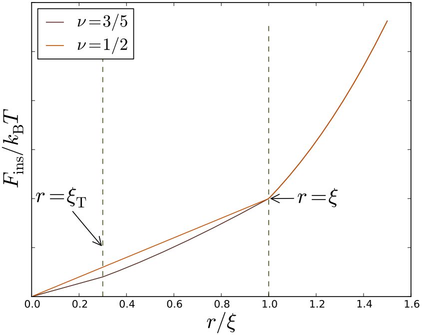

Insertion Mode

Generally,

$$F_{ins} = \Pi(\phi)V + \gamma(\phi)A$$

When $r > \xi$

$$\frac{F_{ins}}{k_B T} \sim \left(\frac{r}{\xi}\right)^3 \left[1 + \frac{\xi}{r}\right]$$

When $r < \xi$

$$\frac{F_{ins}}{k_B T} \sim \left(\frac{r}{\xi}\right)^{3-1/\nu}$$

Concentration Profile

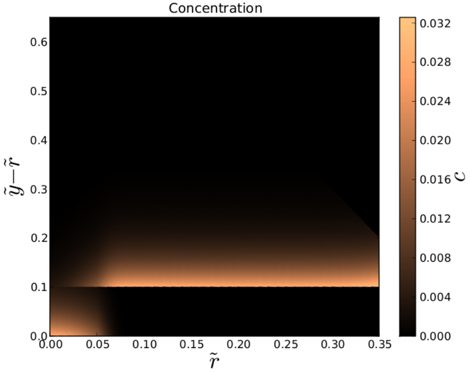

Figure: The piece-wise free energy cost creates abrupt changes in $c(\tilde{y}, \tilde{r})$ such that the concentration plumets when $r < \xi$. For $\lambda = k_B T / fw = 0.05$, $\tilde{H} = 0.1$ and $\tilde{\xi} = 0.05$.

Retention Ratio, $R = \langle \mathcal{V} \rangle / \langle v \rangle$

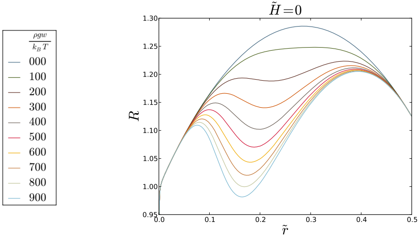

- FFF is nonmonotonic

Retention Ratio, $R = \langle \mathcal{V} \rangle / \langle v \rangle$

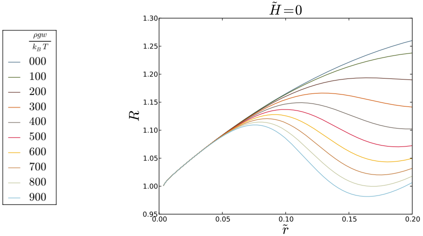

- FFF is nonmonotonic

Retention Ratio, $R = \langle \mathcal{V} \rangle \,/\, \langle v \rangle$

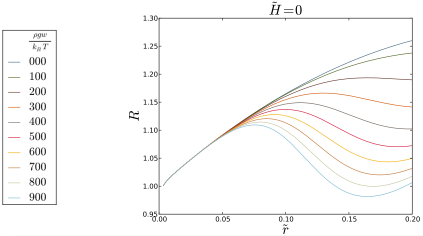

- FFF is nonmonotonic
- Brush makes $R : \tilde{r} \rightarrow 1 : 1$ over larger range

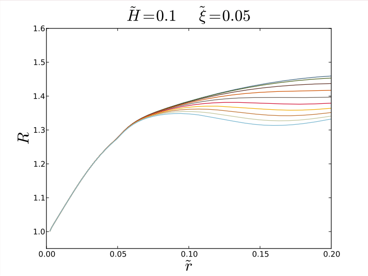

Retention Ratio, $R = \langle \mathcal{V} \rangle \,/\, \langle v \rangle$

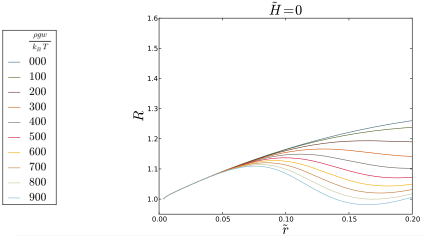

- FFF is nonmonotonic
- Brush makes $R : \tilde{r} \rightarrow 1 : 1$ over larger range
- Dense brush increases resolution

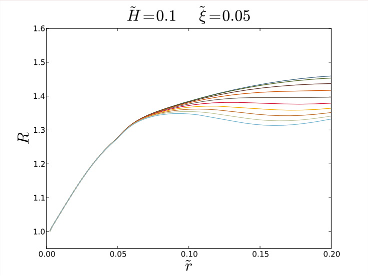

Retention Ratio, $R = \langle \mathcal{V} \rangle \,/\, \langle v \rangle$

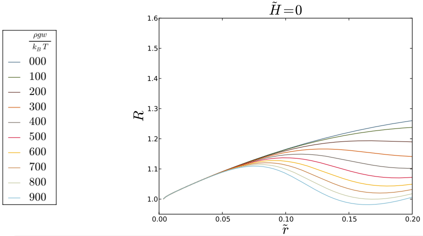

- FFF is nonmonotonic
- Brush makes $R : \tilde{r} \rightarrow 1 : 1$ over larger range
- Dense brush increases resolution

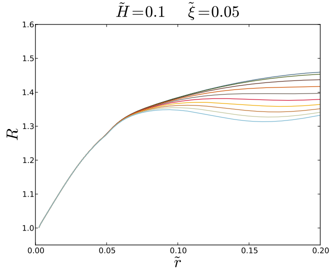

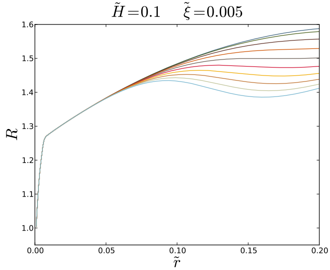

Retention Ratio, $R = \langle \mathcal{V} \rangle \,/\, \langle v \rangle$

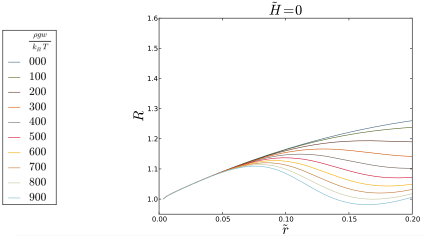

- FFF is nonmonotonic
- Brush makes $R : \tilde{r} \to 1 : 1$ over larger range
- Dense brush increases resolution
- At this size, retention is independent of field

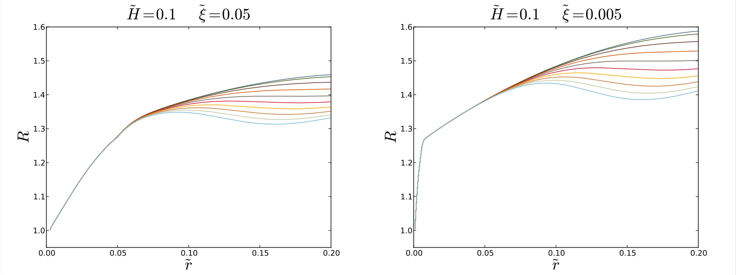

Multi-Particle Collision Dynamics

MPC-MD Hybrid

Ideal for Pé≈ 1

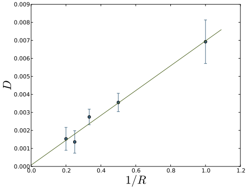

Multi-Particle Collision Dynamics

MPC-MD Hybrid

Ideal for Pé$\approx$ 1

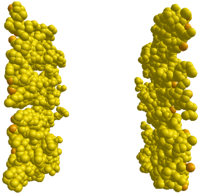

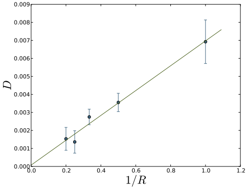

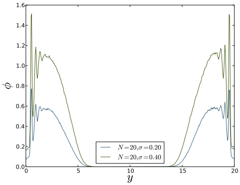

Multi-Particle Collision Dynamics

MPC-MD Hybrid

Ideal for Pé≈ 1

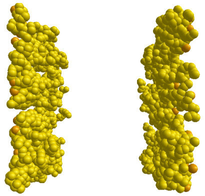

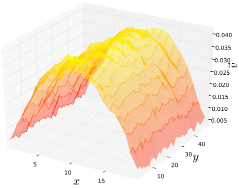

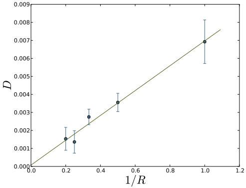

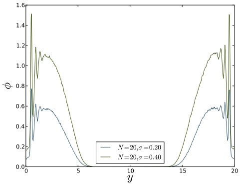

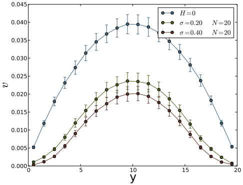

Conclusions

Selective Steric-mode Field Flow Fractionation

- Polymer brush alters FFF by
  - screening flow within the brush
  - enacting free energy cost to enter
- Polymer brush leads to
  - increased monotonic range
  - increased resolution
  - significantly increased resolution of solutes smaller than blobs
- Simple model to be corroborated by MPC-MD simulations

Thank you,

Thank you to the U. of O. Polymer Physics Group members

- Mykyta Chubynsky
- Yugou Tau
- Henk DeHaan
- David Sean
- Owen Hickey

Steric-mode FFF

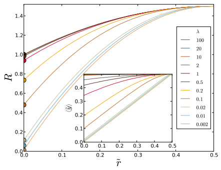

Figure: Retention ratios for fixed retention parameters, λ.

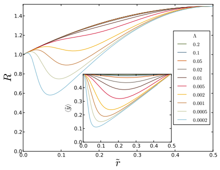

Figure: Retention ratios when force varies with particle size $\lambda = \Lambda \tilde{r}^{-\alpha}$.

$$\lambda = \frac{k_B T}{f w} = \frac{k_B T}{\mu \tilde{r}^{\alpha} w} = \Lambda \tilde{r}^{-\alpha}$$

Snug-mode FFF

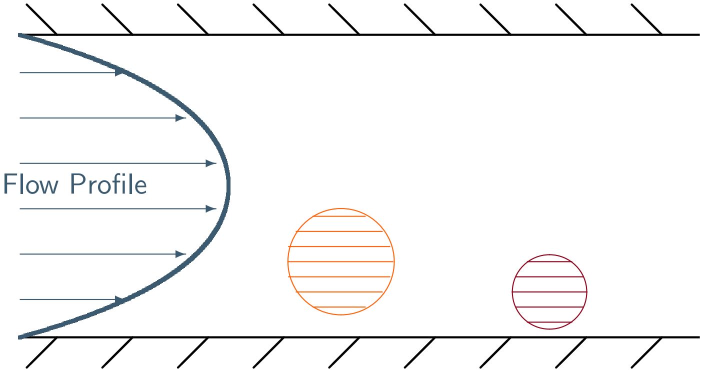

Figure: Schematic of snug-mode FFF.

Snug-mode FFF

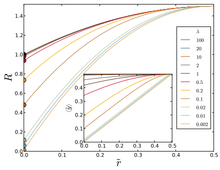

Figure: Retention ratios for fixed retention parameters, λ.

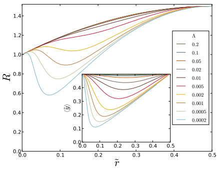

Figure: Retention ratios when force varies with particle size $\lambda = \Lambda \tilde{r}^{-\alpha}$.

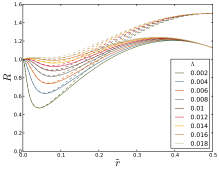

Figure: Retention ratios when velocity profile average over surface area.

Snug-mode FFF

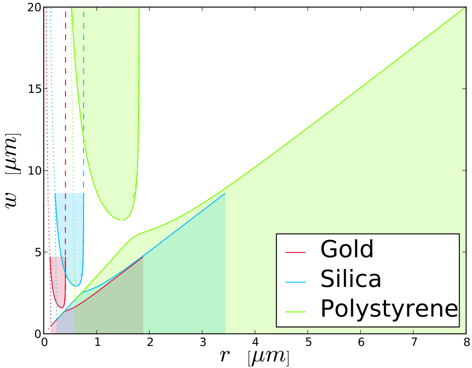

Flow Profile

Brinkman equation:

$$\eta \nabla^2 v + \frac{\eta}{\xi^2} v = \nabla p$$

where ξ is the hydrodynamic penetration depth which acts as the typical pore size and corresponds to the correlation length of the chains.

- Alexander Brush - step function density

$$\xi = \frac{b}{\phi^{\nu/(3\nu-1)}}$$

  L. Miao, H. Guo, M.J. Zuckermann. Conformation of polymer brushes under shear. Macromolecules, 29(6):22892297, 1996.
- Parabolic Brush - density falls linearly at extremity

$$\xi = \frac{b}{\phi}$$

  S. T. Milner. Hydrodynamic penetration into parabolic brushes. Macromolecules, 24(12):37043705, 1991.

Free Energy Coefficients

$$\frac{\Delta F}{k_B T} \sim \begin{cases} F_0 \left[\left(\frac{H}{h}\right)^{1/(3\nu-1)} + \left(\frac{h}{H}\right)^{(1-4\nu)/(1-3\nu)} - 1 \right] & r \gg H \\ \left(\frac{r}{\xi}\right)^3 & H \gg r \gg \xi \\ \left(\frac{r}{\xi}\right)^3 \left[1 + \frac{\xi}{r}\right] & r \geq \xi \\ \left(\frac{r}{\xi}\right)^{3-1/\nu} & \xi > r > \xi_T \\ \frac{r}{\xi_{\text{id}}} & \xi_T > r > b \end{cases}$$

Free Energy Coefficients

$$\frac{\Delta F}{k_B T} \sim \begin{cases} F_0 \left[\left(\frac{H}{h}\right)^{1/(3\nu-1)} + \left(\frac{h}{H}\right)^{(1-4\nu)/(1-3\nu)} - 1 \right] & r \geq H \\ \left(\frac{r}{\xi}\right)^3 \left[1 + \frac{\xi}{r}\right] & \xi \leq r \leq H \\ \left(\frac{r}{\xi}\right)^{3-1/\nu} & r \leq \xi \end{cases}$$

Free Energy Coefficients

$$\frac{\Delta F}{k_\mathrm{B} T} = \begin{cases} a_1 F_0 \left[\left(\frac{H}{h}\right)^{1/(3\nu-1)} + \left(\frac{h}{H}\right)^{(1-4\nu)/(1-3\nu)} - 1 \right] & r \geq H \\ a_2 \left(\frac{r}{\xi}\right)^3 \left[1 + \frac{\xi}{r}\right] & \xi \leq r \leq H \\ a_3 \left(\frac{r}{\xi}\right)^{3-1/\nu} & r \leq \xi \end{cases}$$

Free Energy Coefficients

$$\frac{\Delta F}{k_{\mathrm{B}} T} = \begin{cases} a_1 F_0 \left[\left(\frac{H}{h}\right)^{1/(3\nu-1)} + \left(\frac{h}{H}\right)^{(1-4\nu)/(1-3\nu)} - 1 \right] & r \geq H \\ a_2 \left(\frac{r}{\xi}\right)^3 \left[1 + \frac{\xi}{r}\right] & \xi \leq r \leq H \\ a_3 \left(\frac{r}{\xi}\right)^{3-1/\nu} & r \leq \xi \end{cases}$$

Recalling $F_0 = H/\xi$. At $r = H$, $F_1 = F_2$ such that

$$a_1 = a_2 \left(\frac{H}{\xi}\right)^2 \left[1 + \frac{\xi}{H}\right]$$

At $r = \xi$, $F_2 = F_3$ and we see

$$a_3 = 2a_2$$

We choose $a_2 = 1$.